PHYSICAL REVIEW B **66**, 020404(R) (2002)

Self-assembled one-dimensional magnetic Ising chains: Co/Ru(0001)

Dongqi Li, Chengtao Yu, J. Pearson, and S. D. Bader
Materials Science Division, Argonne National Laboratory, Argonne, Illinois 60439
(Received 10 May 2002; published 28 June 2002)

Self-assembled Co dot chains were epitaxially grown on Ru(0001) along grooves and were characterized with atomic- and magnetic-force microscopies, and the-magneto-optic Kerr effect. The dots are of order 100 nm in diameter and 1–7 nm high and have magnetic single domains with in-plane uniaxial anisotropy along the grooves. The interdot pair correlation along a chain was deduced experimentally from the magnetic-force microscopy images, and can be understood in terms of the classical one-dimensional Ising model.

DOI: 10.1103/PhysRevB.66.020404 PACS number(s): 75.75.+a, 68.65.−k, 75.10.Hk, 75.30.Gw

As nanoscale magnetic materials are attracting extensive interest, various self-assembly techniques are becoming viable tools for their fabrication. One type of approach is to employ molecular-beam epitaxy (MBE), traditionally used for two-dimensional (2D) films, and to utilize unique surface phenomena such as step decoration,[1–4] surface strain,[5,6] and reconstructed surfaces as templates[7,8] to assemble lateral structures. The resultant magnetic nanostructures, as well as their organization, promise unique magnetic properties and can serve as model systems to explore low-dimensional physics. To date, 1D behavior has mostly been investigated via macroscopic measurements such as magnetic susceptibility and neutron scattering in bulk compounds with chain structures.[9–11] Recent developments in nanoscience make it possible to fabricate and probe *artificial* quasi-1D systems such as nanowires made via step decoration.[2–4] The individual spins in these step-induced nanowires, however, are still not resolved. A model low-dimensional system with lateral magnetic dot chains or other arrays permit the visualization of individual ''spin'' units and therefore directly probe microscopic properties, such as the pair correlation function, through statistical analysis. This requires that the dots remain in single domains and act as one unit. In addition, to experimentally observe a pair correlation that clearly deviates from 0 or 1, the dots should couple with each other on an energy scale comparable to the experimental temperatures. While single-domain states have been widely observed, the expected magnetostatic coupling[12] among dots in submicron magnetic dot arrays has not been observed until recently,[13–16] possibly because such an interaction in submicron chains/arrays is small especially when the dots are not closely spaced.[17] In addition, Cowburn and Welland[15] proposed to use such magnetic dot chains for quantum computing, which makes the issue of understanding dot chains even more urgent and of general interest.

Recently, we reported the self-assembly of Co dots, antidots, dot chains, and stripes on Ru(0001) by MBE at elevated temperature.[18,19] These structures, typically ~70–500 nm in lateral scale and relatively uniform in size for a given coverage, are mainly driven by the lattice mismatch and therefore strain in epitaxy analogous to the semiconductor quantum dots that have been widely studied in recent years.[20] In the present work, we demonstrate that Co dot chains, formed along grooves in a Ru(0001) substrate, appear to be a classical Ising chain since the dots have single domains with uniaxial anisotropy and are weakly coupled ferromagnetically. The nearest-neighbor correlation among the dots is experimentally measured and modeled in terms of a 1D Ising chain. With the increasing popularity of various imaging techniques, such experimental methodology in deducing properties such as correlation function from real space can be widely used in the future.

Co was deposited onto flat and grooved Ru(0001) substrates at 350 °C via MBE in a wedge configuration with nominal thickness ranging from 0 to 10 nm across the substrate in an ultrahigh vacuum chamber with a base pressure of 1×10^{-10} Torr. The Ru grooves with asymmetric sawtooth profile were formed due to residual directional mechanical polishing lines or step bunching, with spacings of ~1 μm and depths around 10 nm [see Fig. 1(b)]. The substrates were cleaned *in situ* by cycles of annealing in O_2 and flashing.[21] Both the substrates and the Co dots are clean and well ordered as confirmed with low-energy electron diffraction and Auger spectroscopy. The morphology and micromagnetic properties of the samples were measured *ex situ* with atomic force microscopy (AFM) and magnetic force microscopy (MFM). The global magnetic properties were characterized *ex situ* by means of the longitudinal magneto-optic Kerr effect (MOKE) at different azimuthal angles.

Figure 1(a) shows a typical 3D AFM image of the self-assembled Co dots on the grooved Ru(0001) for a nominal thickness of 0.8 nm. The dots are ~280 nm in diameter and ~3.4 nm in height, which are typical dimensions for this study. In general, the dots are of order 100 nm in diameter and 1–7 nm high depending on different coverage. The dots align into chains along the top and bottom of the grooves, even though they tend to distribute uniformly on a flat Ru(0001) surface, as seen in the inset.[18] (Note that the *z* scale of the image is exaggerated to emphasize the groove structure and the shape of the dots.) Interestingly, more dots stay on top than at the bottom. Figure 1(b) is a schematic cross section perpendicular to the grooves. It shows the locations of the dot chains with respect to the grooves, and the profiles of the dots. While the dots show the quasihexagonal shape in plan view,[18,19] their profiles are asymmetric perpendicular to the grooves, with their top surfaces parallel to one side of the grooves. This is a result of keeping the growth front of the dots in the basal plane [0001] direction.[19] Different arrangements, such as single chains, double chains, and stripes, were observed depending on details of the coverage and substrate profile.

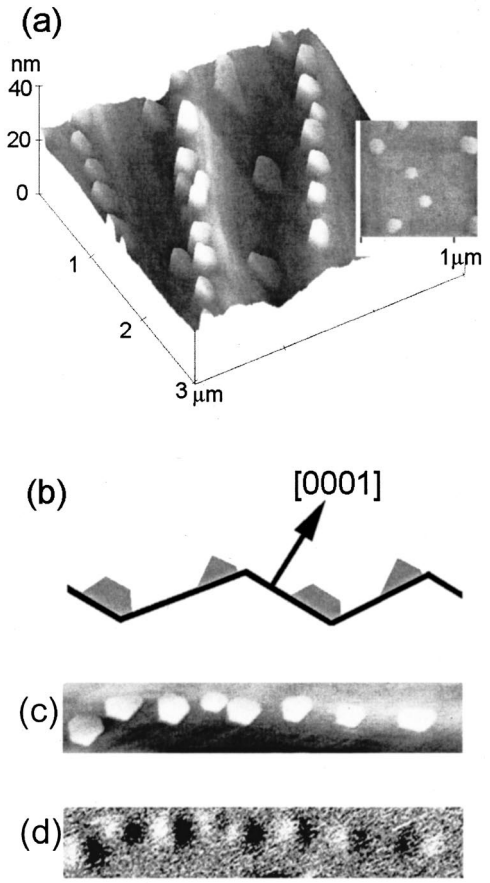

FIG. 1. (a) Typical 3D image of the dot chains along the top and bottom edges of the grooves on Ru(0001) at a nominal thickness of 0.8 nm. Note that the dots are tilted with their top parallel to one side of the groove. The inset is an AFM plan view of the dots on a flat substrate. (b) Schematics of the location and shape of the dots on the grooved substrate. (c) AFM and (d) the corresponding MFM images of one magnetic dot chain in (a). Note that the moments of the dots tend to point to the same direction, indicating a ferromagnetic coupling among the dots in a chain.

Figures 1(c) and 1(d) show the plan view of the corresponding AFM and MFM images of a typical dot chain from Fig. 1(a). In their virgin state, the dots are half-dark and half-bright in the MFM images. Since MFM is sensitive to the field gradient perpendicular to the surface, this contrast indicates the poles of an in-plane single domain state. While the moments of the dots are observed to randomly point to any of the 12 high-symmetry directions on flat substrates, they align along the grooves in dot chains and stripes. This suggests a uniaxial magnetic anisotropy with easy axis along the chains.

Such an anisotropy of the dot chains and stripes is indeed confirmed by the macroscopic longitudinal MOKE measurements in Fig. 2. We collected loops with the sample rotated azimuthally before each magnetic measurement, as shown schematically in Fig. 2(a). Figure 2(b) shows a polar plot of the angular dependence of the remanent magnetization M_R at a nominal thickness of 5 nm. Along the grooves or the chains/stripes (0°), the M_R is maximal, indicating an easy axis. Perpendicular to the grooves (90°), the M_R is minimal,

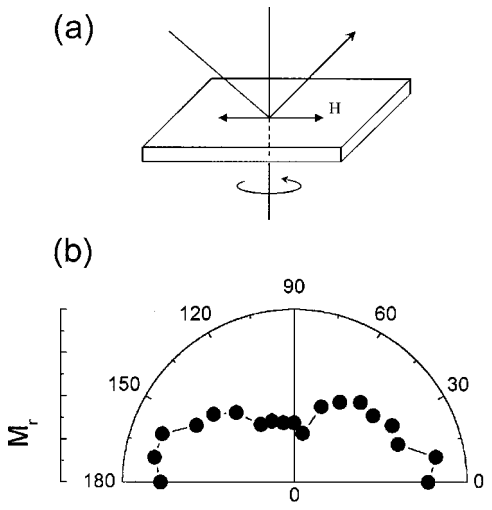

FIG. 2. (a) Schematic experimental geometry for longitudinal MOKE measurements, as the sample is rotated around its normal before each measurement. (b) Remanent magnetization as a function of the azimuthal angle. The error bar is about twice the dot size. The magnetization shows twofold symmetry, indicating a uniaxial magnetic anisotropy.

indicating a hard axis. The results indicate a twofold symmetry, which confirms the existence of a uniaxial anisotropy. The angular dependence of the magnetic anisotropy becomes weaker for larger coverage as the stripes start to connect into a continuous film, and is not observed in corresponding samples of flat Ru(0001). We attribute the uniaxial anisotropy mainly to the anisotropic strain due to the grooves, though magnetostatic interactions in a closely spaced dot chain or a stripe should also contribute.[17]

In addition to the uniaxial anisotropy, it is also evident in Fig. 1(d) that the neighboring moments in closely spaced dot chains exhibit a great tendency to point in the same direction. No globally preferred magnetization direction, however, was observed when averaging over many chains in a large area in the virgin state. This rules out the external field as the possible origin for the magnetic alignment along the chains. This alignment, therefore, indicates a ferromagnetic coupling among the dots that is effective at a length scale of $\sim 10^1 - 10^2$ nm. This is the result of interdot magnetostatic interactions, which favors a ferromagnetic alignment of the moments along the chain. Indeed, magnetic couplings have recently been observed in magnetic dot arrays of similar length scale.[13,14]

By examining all the MFM images collected for the dots of ~280 nm in diameter and ~3.4 nm in height, the probabilities of nearest-neighbor dots with parallel and antiparallel moments, $P_{\uparrow\uparrow}$ and $P_{\uparrow\downarrow}$ are plotted in Fig. 3 as a function of their center-to-center distance. Parallel pairs of nearest neighbors greatly out-number the antiparallel ones, confirming the ferromagnetic coupling among dots. The existence of the peaks as a function of pair distance reflects that the dots tend to be uniformly distributed along the chains. The peak for parallel pairs is at ~430 nm, while that of the antiparallel pairs is at ~490 nm. This hints that the coupling is stronger when the dots are closer to each other.

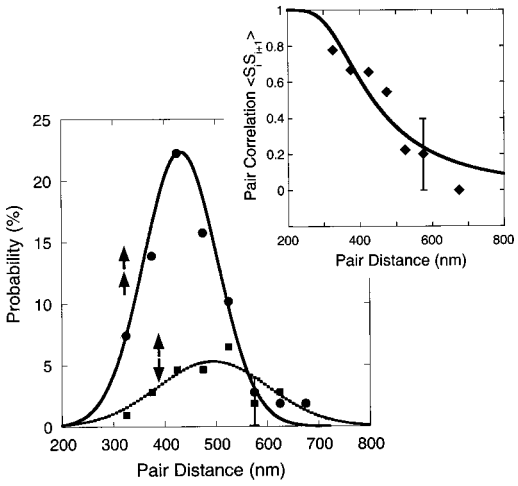

FIG. 3. Probability of the nearest-neighbor dots (pairs) in parallel (●) or antiparallel (■) alignment as a function of pair distance. The pairs with similar distances are grouped into bins 50 nm wide. The lines are fittings with Gaussian functions and are the guides to the eye. In the inset, the diamond symbols (♦) shows the experimental pair correlation function derived from the probability data, while the solid line is a fit with the pair correlation function of a 1D Ising model, as discussed in the text.

The probabilities for parallel and antiparallel neighbors can also be described by a pair correlation function, which is experimentally derived (diamonds) and fitted (solid line), in the inset of Fig. 3. Since the dots have similar sizes and are single domains, we assume that the total moment of each dot is fixed at the same value and can only point in two opposite directions as dictated by the uniaxial anisotropy. We can then define the state of the dot on site i with its direction, i.e., $S_i=+1$ or -1. The nearest-neighbor pair correlation function can therefore be deduced as

$$\langle S_i S_{i+1}\rangle = \frac{P_{\uparrow\uparrow}-P_{\uparrow\downarrow}}{P_{\uparrow\uparrow}+P_{\uparrow\downarrow}}, \tag{1}$$

which is plotted in the inset of Fig. 3. The decrease in correlation as the pair distance increases further illustrates that the magnetic interdot interaction decreases with increasing distance as one expects.

We can model the system with a classical 1D Ising chain at zero field. The pair correlation function of the spins at sites i and $i+j$ in such a model system is exactly solved as[22,23]

$$\langle S_i S_{i+j}\rangle = [\tanh(\beta J)]^j, \tag{2}$$

where J is the coupling constant and β is $1/(k_B T)$. The nearest-neighbor correlation is therefore

$$\langle S_i S_{i+1}\rangle = \tanh(\beta J) = \tanh\left(\frac{E_{\uparrow\downarrow}-E_{\uparrow\uparrow}}{2k_B T}\right), \tag{3}$$

where $E_{\uparrow\uparrow}$ and $E_{\uparrow\downarrow}$ are the energies of dot pairs with parallel and antiparallel alignment, respectively. Approximating the magnetostatic interaction as being dipolar, i.e., $E_{\uparrow\downarrow}-E_{\uparrow\uparrow}=4m_i m_{i+1}/r^3$, we fitted the experimental data (Fig. 3 inset) with

$$\langle S_i S_{i+1}\rangle = \tanh\left(\frac{A}{r^3}\right), \tag{4}$$

where $A=2m_i m_{i+1}/kT$, and m_i is the total moment of the dot at site i. Assuming that $m_i=m_{i+1}$, the resulting fitting parameter is $m_i=4.5\times10^{-14}$ emu. This corresponds to a hexagonal Co dot of 160 nm in diameter and 2 nm in height, given the bulk value of the Co saturation magnetization. Comparing to the measured average dot size of ~280 nm in diameter and 3.4 nm in height, the theoretical analysis reasonably agrees with the experimental data, in spite of the approximations and assumptions. This fit indicates that the 1D Ising model describes the basic physics of the magnetic Co dot chains. The fact that the interdot interaction in the dot chains at this length scale is comparable to the thermal energy at the experimental temperatures makes it possible to show the effects of thermal excitation and therefore a pair correlation between 0 and 1.

In principle, the dots should be described as micromagnetic objects instead of simple dipoles. Detailed micromagnetic calculations for these systems, as an independent study, are to be published elsewhere,[17] where the magnetic states of single dots and dot pairs are investigated. Micromagnetic modeling indicates that the single-domain state is quite stable. And the total moment does not vary significantly for a given dot during magnetization reversal. In other words, it is reasonable to view each dot as a fixed moment that can align along two opposite directions, which is a key assumption of the current analysis. The interdot magnetostatic interaction also deviates from the dipolar approximation especially when the pair distance is small.[17] A fit with the corrected magnetostatic interaction, however, gives rise to a similar fitting curve and does not qualitatively change our understanding of the system.

It is well known that an infinite 1D Ising chain does not have long range order, i.e., $\lim_{j\to\infty}\langle S_i S_{i+j}\rangle=0$. Our data confirm, however, that ferromagnetic correlation indeed exists at short range even in our 1D system presumably because ferromagnetic coupling is present. Within a finite length, the chains appear to be magnetically ordered with sizable total magnetization, as seen in Fig. 1(d). Since all quasi-1D systems have finite length, this in itself acts to break the symmetry and permits the ordering. Indeed, Fe stripes on stepped Pd(110) exhibit ferromagnetic hysteresis loops with full remanence, even though their magnetization and coercivity field exhibit anomalous temperature dependences.[4]

It is interesting to note that, in an antiferromagnetically coupled dot chain by Cowburn,[16] the ordering only persist among 4–5 dots in its demagnetized state. This is consistent with our results that only short-range order exists in 1D chains at zero-field. For a ferromagnetically coupled chain under a finite field,[15] however, the dots can be 90% aligned among 69 dots. Indeed, a 1D Ising chain *should* be strongly affected by magnetic field with the moments progressively aligned along the increasing field.[22,23] It would be interesting to further investigate field dependence of the dot chains in the future.

In conclusion, we have grown magnetic dot chains on

grooved Ru(0001) at elevated temperature via self-assembly. This suggests that complex and functional arrangements should be realizable by performing self-assembly growth on substrates with lithographically defined patterns. These dot-chains have unique magnetic properties, such as uniaxial magnetic anisotropy along the chains, and ferromagnetic pair correlation. The correlation is understood with a 1D Ising model. In the future, it would be interesting to further utilize these dot chains and other lateral nanostructures as model systems to investigate low-dimensional physics.

This work was supported by DOE BES under contract No. W-31-109-ENG-38.

[1] F. J. Himpsel, T. Jung, and J. E. Ortega, Surf. Rev. Lett. **4**, 371 (1997).

[2] J. Hauschild, H. J. Elmers, and U. Gradmann, Phys. Rev. B **57**, R677 (1998).

[3] J. Shen, M. Klaua, P. Ohresser, H. Jenniches, J. Barthel, C. V. Mohan, and J. Kirschner, Phys. Rev. B **56**, 11 134 (1997).

[4] Dongqi Li, B. Roldan Cuenya, J. Pearson, S. D. Bader, and W. Keune, Phys. Rev. B **64**, 144410 (2001); B. Roldan Cuenya, J. Pearson, Chengtao Yu, Dongqi Li, and S. D. Bader, J. Vac. Sci. Technol. A **19**, 1182 (2001).

[5] H. Röder, E. Hahm, H. Brune, J.-P. Bucher, and K. Kern, Nature (London) **366**, 141 (1993); H. Brune, K. Bromann, H. Röder, K. Kern, J. Jacobsen, P. Stoltze, K. Jacobsen, and J. Nørskov, Phys. Rev. B **52**, R14 380 (1995).

[6] E. D. Tober, R. F. C. Farrow, R. F. Marks, G. Witte, K. Kalki, and D. D. Chambliss, Phys. Rev. Lett. **70**, 3943 (1993).

[7] Dongqi Li, V. Diercks, J. Pearson, J. S. Jiang, and S. D. Bader, J. Appl. Phys. **85**, 5285 (1999).

[8] D. D. Chambliss, R. J. Wilson, and S. Chiang, Phys. Rev. Lett. **66**, 1721 (1991).

[9] M. Steiner, J. Villain, and C. G. Windsor, Adv. Phys. **25**, 87 (1976).

[10] For example, M. Kohgi, K. Iwasa, J.-M. Mignot, B. Fåk, P. Gegenwart, M. Lang, A. Ochiai, H. Aoki, and T. Suzuki, Phys. Rev. Lett. **86**, 2439 (2001); H. Woll, M. C. Rheinstädter, F. Kruchten, K. Kiefer, M. Enderle, A. Klöpperpieper, J. Albers, and K. Knorr, Phys. Rev. B **63**, 224202 (2001); R. S. Rubins, A. Sohn, T. D. Black, and J. E. Drumheller, *ibid.* **61**, 11 259 (2000); S. Kobayashi, S. Mitsuda, M. Ishikawa, K. Miyatani, and K. Kohn, *ibid.* **60**, 3331 (1999); K. Kojima, A. Keren, L. P. Le, G. M. Luke, B. Nachumi, W. D. Wu, Y. J. Uemura, K. Kiyono, S. Miyasaka, H. Takagi, and S. Uchida, Phys. Rev. Lett. **74**, 3471 (1995).

[11] D. J. García, K. Hallberg, C. D. Batista, M. Avignon, and B. Alascio, Phys. Rev. Lett. **85**, 3720 (2001); W. Koshibae, M. Yamanaka, M. Oshikawa, and S. Maekawa, *ibid.* **82**, 2119 (1999); J. Riera, K. Hallberg, and E. Dagotto, *ibid.* **79**, 713 (1997).

[12] M. Grimsditch, Y. Jaccard, and I. K. Schuller, Phys. Rev. B **58**, 11 539 (1998); K. Yu. Guslienko, Appl. Phys. Lett. **75**, 394 (1999).

[13] M. C. Abraham, H. Schmidt, T. A. Savas, H. I. Smith, C. A. Ross, and R. J. Ram, J. Appl. Phys. **89**, 5667 (2001).

[14] V. Novosad, K. Yu. Guslienko, Y. Otani, H. Shima, S. G. Kim, and K. Fukamichi, Phys. Rev. B **65**, 060402 (2002).

[15] R. P. Cowburn and M. E. Welland, Science **287**, 1466 (2000).

[16] R. P. Cowburn, Phys. Rev. B **65**, 092409 (2002).

[17] For micromagnetic calculation of such a coupling, see, for example, Chengtao Yu, J. Pearson, and Dongqi Li, J. Appl. Phys. **91**, 6955 (2002).

[18] Chentao Yu, Dongqi Li, J. Pearson, and S. D. Bader, Appl. Phys. Lett. **78**, 1228 (2001).

[19] Chengtao Yu, Dongqi Li, J. Pearson, and S. D. Bader, Appl. Phys. Lett. **79**, 3848 (2001).

[20] P. Politi, G. Grenet, A. Amarty, A. Ponchet, and J. Villain, Phys. Rep. **324**, 271 (2000), and references therein.

[21] R. G. Musket, W. Mclean, C. A. Colmenares, D. M. Makowiecki, and W. J. Siekhaus, Appl. Surf. Sci. **10**, 143 (1982).

[22] E. Ising, Z. Phys. **31**, 253 (1925).

[23] See, for example, C. J. Thompson, in *Phase Transitions and Critical Phenomena*, edited by C. Domb and M. S. Green (Academic Press, London, 1972), Vol. 1, p. 177.